(please add to chapter " gastric cancer")

Table 6 Five genes for predicting risk of lymphnode metastasis in intestinal gastric cancer (Hasegawa 2002)

Title		Discriminant coefficient
DDOST	dolichyl-diphosphooligosaccharide-protein glycosyltransferase	1.87
GNS	glucosamine (N-acetyl)-6-sulfatase (Sanfilippo disease IIID)	1.26
NEDD8	neural precursor cell expressed, developmentally down-regulated 8	1.29
LOC51096	CGI-48 protein	1.36
AIM2	absent in melanoma 2	-1.54

Five genes were selected based on microarray data for predicting risk of lymph-node metastasis in intestinal gastric cancer (Hasegawa 2002).This "predictor" was validated in 9 additional independent cases. All cases were (four node positive and five node negative) were assigned to each classes.

(please add to chapter " lymphoma")

Table 7 Model of 13 genes predicting outcome in DLBCL Patients (Shipp 2002)

Genes associated with good outcome	Genes associated with poor outcome
-Dystrophin related protein 2	-H731
-3UTR of unknown protein	-Transduction like enhancer protein 1
-uncharacterised	-PDE 4 B
-Protein Kinase C gamma	-uncharacterised
-Minor / NOR 1	-Protein kinase C beta 1
-Hydroxitryptamine 2B Receptor	-Oviductal glycoprotein
-Zinc finger protein C2H2-150	

A 13-gene based "predictor" for outcome in DLBCL patients was developed based on microarray data by a supervised learning method (Shipp 2002). The expression of seven genes were associated with good and the expression of six genes was associated with poor outcome. This "predictor" was superior to "hierarchical clustering" based classification of Alizedah in predicting outcome of DLBCL patients.

Table 8 Analysis of microarray based correlation studies (1999-2003) by Nitani and Ioannidis (Nitani 2003) (please add chapter Relability and.. "

Characteristic	Studies of major clinical outcomes (n=30)	Other studies (n=54)	Total (n=84)
Year of publication			
1999	1(3%	2(4%	3(4%
2000	2(7%	1(2%	3(4%
2001	6(20%	18(33%	24(29%
2002	18(60%	28(52%	46(55%
2003	3(10%	5(9%	8(10%
Malignant disorder			
Haematological	9(30%	9(17%	18(21%
Solid tumor	21(70%	45(83%	66(79%
Median (IQR) number of samples			
Total	62(29-96)	30(18-44)	37(20-57)
Specific cancer	43(24-69)	20(13-36)	25(15-45)
Microarray type			
cDNA	19(63%	31(57%	50(60%
Oligonucleotide	11(37%	23(43%	34(40%
Median (IQR) number of probes	8683 (6817-18 624)	6936 (4569-12 600)	7014 (5534-12 600)
Training			
Independent	9(30%	17(32%	26(31%
Dependent	8(27%	20(37%	28(33%
Both	13(43%	17(32%	30(36%
Validation			
Independent	3(10%	1(2%	4(5%
Cross-validation	6(20%	4(7%	10(12%
Both	3(10%	5(9%	8(10%
None	18(60%	44(82%	62(74%
Outcomes/correlates assessed			
One	9(30%	35(65%	44(52%
Two to four	12(40%	11(20%	23(27%
Five or more	9(30%	8(15%	17(20%
Significant associations reported			
Yes	21(70%	20(37%	41(49%
No	9(30%	34(63%	43(51%

Microarray correlation studies focused on prediction outcome or other impotent clinico-pathological features were systematically analysed by Nitani and Ioannidis in 2003. This table shows the results of their investigations. In 70% of the studies co rrelating major clinical outcome with gene expression significant associations were reported. However, in only 30 percent of the major outcome focused studies cross-validation or independent validation was performed. These findings underline the need for conseqent quality control and vali dation in microarray based clinical studies.

Figure legends

Fig. 1. Clustering of gene expressions of tissues 3 from lung cancer patients (Ohira 2002). Tumor tissue and normal lung tissue was collected while surgery after neoadjuvant chemotherapy. Tumor tissue and normal tissue from the same patient show more similarities and clustered nearer than normal

Fig. 2. Histogram of gene expression profile of lung cancer tissue. Expression profile of cancer tissues as compared with normal tissues.

Case B; increased expression of the genes related to cell cycle regulator, intermediate filaments, adhesion motility and angiogenesis in the tumor tissues. Expression of the other gene group were decreased in tumor tissue. Case C; increased expression of genes related with cell cycle, adhesion were observed in the tumor tissue. Decreased expression of growth factor and cytokine related genes were also observed in tumor of Case C. Taken together, the expression profile of lung carcinoma could be characterized by the increased expression of the genes related with adhesion motility and angiogenesis.

Fig. 3(A). Average-linkage hierarchical clustering analysis of ten colorectal tumor samples on histological diagnosis. Right cluster shows the group of the well-differentiated and left shows the group of the other differentiations. (B) Principal component analysis on histological diagnosis. The numbers in blue indicate the patients with well-differentiated adenocarcinoma and the numbers in red indicate the patients with the other differentiations. The c-myc binding protein gene and the c-jun proto oncogene were identified as possible markers for histological differentiation.

Fig. 4. Macroarray analysing of the 21 samples including PCNSCL, Glioblastoma, Oligodendroglioma and normal tissue. The phylogenetic tree obtained by application of the " clustering algorithm shows separation of the PCNSL.

Fig. 5 . Re-clustering was performed using selected genes related with to response to chemo-radiotherapy.The responders (described as GOOD) and non-responders (described as POOR) were clearly separated clearly by the re-clustering method.

Fig. 6. Gene amplification by T7-based RNA amplification method. In a 2 step approach first cDNA was synthesized (RNA→DNA) followed by c.a.RNA synthesis (DNA→RNA) we could purify 10-100μg RNA of amplified cRNA from small amount of total RNA (1μg or less).

Fig. 7. Is differential expression conserved even after amplification? In order to analyze the reproducibility of the clinical samples, the gene expression profile of non-amplified and amplified samples were compared in scattered plot. Upper: gene expression data of duplicate samples of peripheral blood mononuclear cells were compared in scattered blot. High reproducibility (R=0.93) was obtained. These reproducible profiling was also observed in the amplified samples (R= 0.91). Lower: In a second experiment we compared the differential gene expression of the PC 14 cell line and of peripheral blood mononuclear cells using mRNA and after amplification a.cRNA (amplified cRNA). Also the reproducible profiling was lower after amplification (R=0.50) than in non-amplified samples (R=0.83) we could conserve significant differences in gene expression after amplification.

Fig. 8. Experimental design: sampling of PBL and tissue samples in correlative study in clinical phase I study of a falnesyltransferase inhibitor (FTI). . Peripheral Blood Lymphocytes and tumor samples were collected predose, post-dose day 2 and post dose day 8. Gene alteration after administration of FTI was analyzed for proof the pharmacodynamic effect of FTI.

Fig.9a The cDNA filter-array with a set of 775 genes chosen for predicting chemosensitivity analysis Fig. 9b. Gene expression change of tumor tissue and PBL in the melanoma patient after administration of FTI . Specific gene groups were modulated by FTI. Changes in gene expression influenced by FTI were not only observed in the tumor samples but also in the peripheral blood lymphocytes. This findings suggest that drug modulated changes of gene expression in peripheral blood lymphocytes could be useful as surrogate markers in pharmacogenomic studies.

Fig. 1

Pt. C (Normal Tissues)
Pt. C (Cancer Tissues)
Pt. B (Normal Tissues)
Pt. B (Cancer Tissues)
Pt. A (Normal Tissues)
Pt. A (Cancer Tissues)

Fig. 2

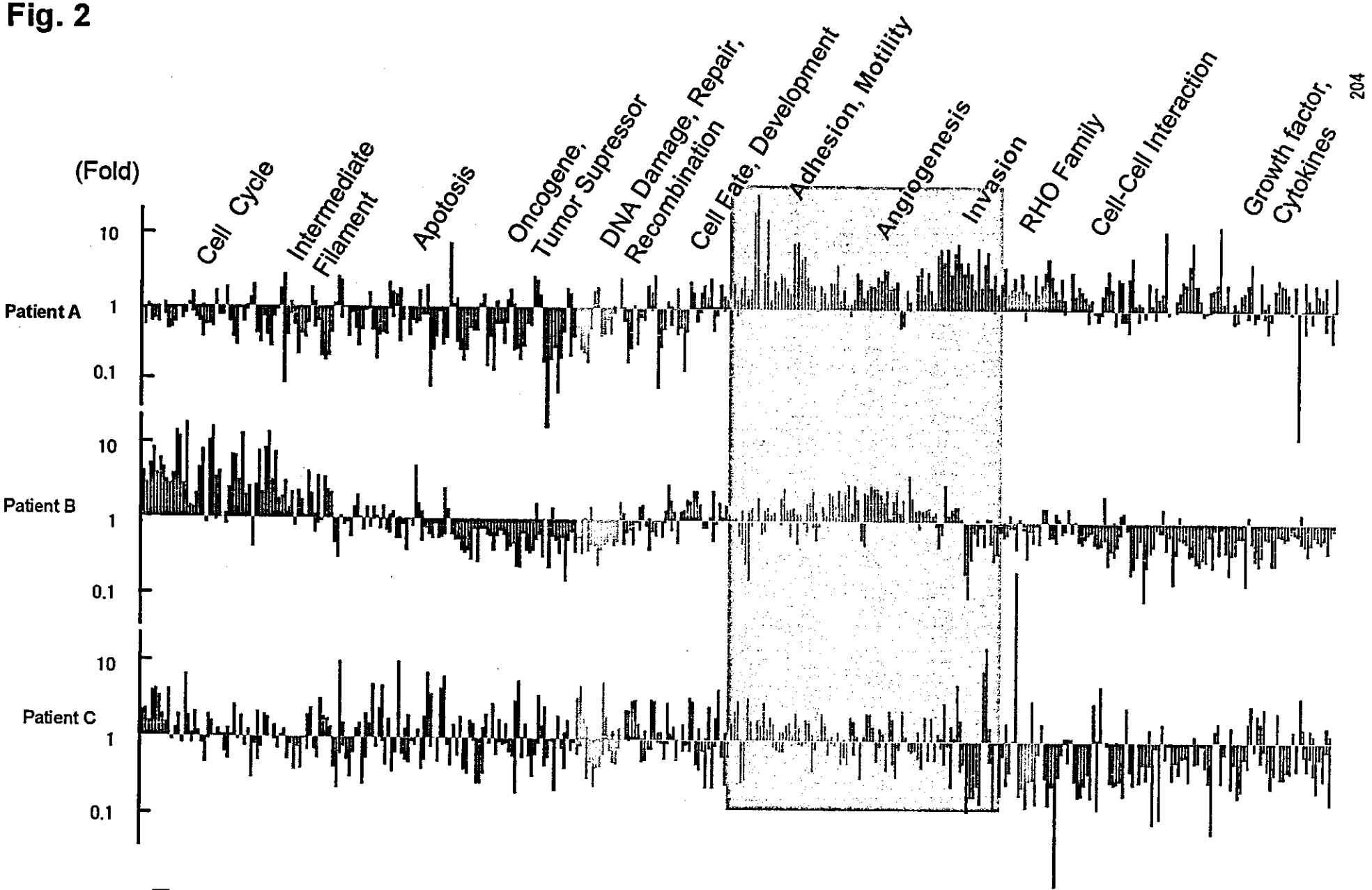

Expression profile of cancer tissues as compared with normal tissues.

Fig 3A

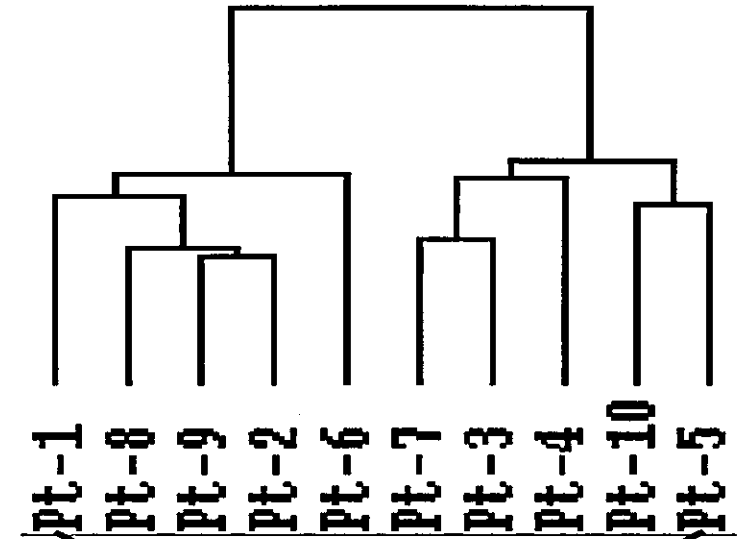

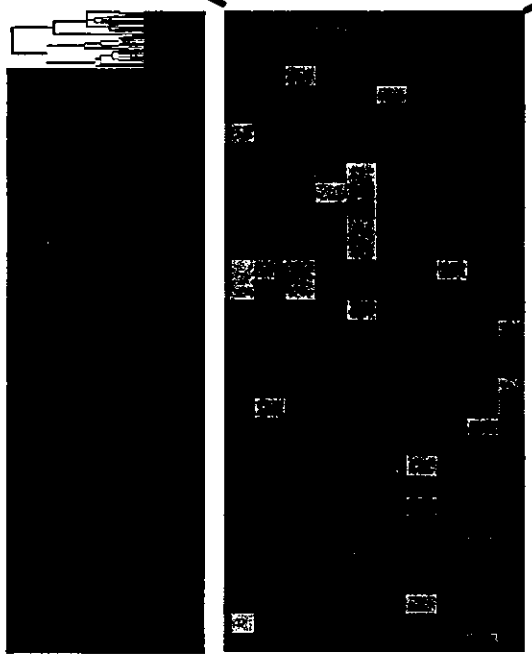

stathmin: phosphoprotein p19 (PP19); oncoprotein 18 (OP18); leukemia-associated phosphoprotein p18 (LAP18); prosolin; metablastin
DNA cytosine-5-methyltransferase (DNA metase; MCMT)
G1/S-specific cyclin E (CCNE)
protein kinase C gamma type (PKC-gamma)
cyclin-dependent kinase 4 inhibitor 2B (CDKN2B); p14-INK4B; multiple tumor suppressor 2 (MTS2)
mitogen-activated protein kinase kinase 7 (MAP kinase kinase 7; MAPKK7; MAP2K7; PRKMK7); MAPK/ERK kinase 7 (MEK7); c-jun N-terminal kinas
cytochrome P450 IIC8 (CYP2C8); mephenytoin 4-hydroxylase
DNA mismatch repair protein MSH2
serum- & glucocorticoid-regulated serine/threonine protein kinase (SGK)
B-raf proto-oncogene (RAFB1)
metastasis-associated protein 1 (MTA1)
mitogen-activated protein kinase kinase 2 (MAP kinase kinase 2; MAPKK2; MAP2K2; PRKMK2); MAPK/ERK kinase 2 (MEK2)
ubiquitin-conjugating enzyme E2D 3 (UBE2D3); UBCH5C
early growth response protein 1 (EGR1); transcription factor ETR103; RNF24; zinc finger protein 225 (ZNF225); RT225
TRAF-interacting protein (I-TRAF) + TRAF family member-associated NF-kappaB activator TANK
colorectal mutant cancer protein (MCC)
sulfonylurea receptor (SUR); ATP-binding cassette subfamily C (CFTR/MRP) member 8 (ABCC8)
microtubule-associated protein 1B
ATP-binding cassette subfamily C member 3 (ABCC3); multidrug resistance-associated protein 3 (MRP3)
anthracycline resistance-associated protein (ARA)
microsomal glutathione S-transferase 1 (MGST1); GST12
fibroblast growth factor 3 (FGF3); HBGF3; int2 proto-oncogene precursor
ataxia telangiectasia (ATM)
mitogen-activated protein kinase kinase 4 (MAP kinase kinase 4; MKK4; PRKMK4); c-jun N-terminal kinase kinase 1 (JNKK1); JNK-activating)
protein kinase C epsilon type (PKCE-epsilon)
ribosomal protein kinase B (RSKB)
coagulation factor VIIIc procoagulant component (F8C)
cyclin-dependent kinase 5 activator isoform p39I precursor (CDK5 activator; NCK5AI)
cadherin 11 precursor (CDH11); osteoblast-cadherin (OB-cadherin); OSF4
mitogen-activated protein kinase kinase 6 (MAP kinase kinase 6; MAPKK6; MAP2K6; PRKMK6); MAPK/ERK kinase 6 (MEK6); SAPKK3
fatty acid synthase
retinoblastoma-related protein p107
CDC6-related protein

Fig 3B

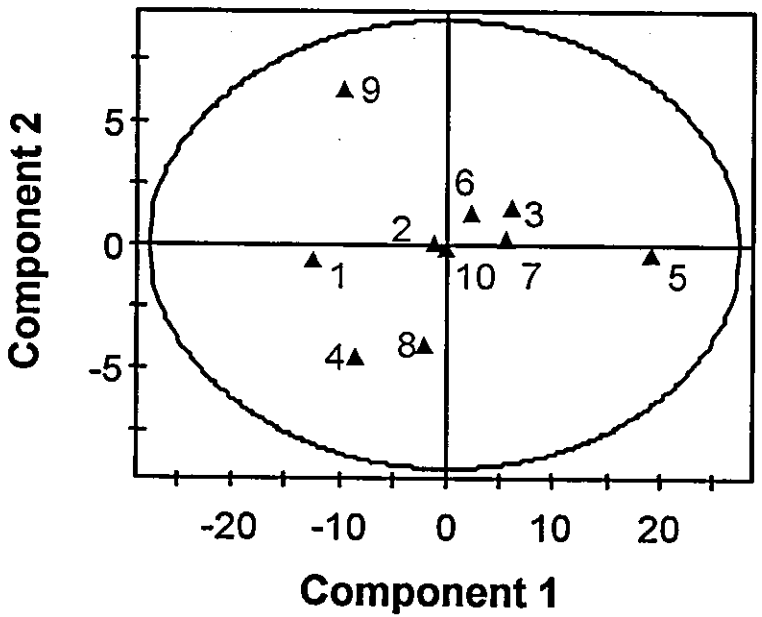
Component 2
5
0
-5
9
6
3
2
1
10
7
5
4
8
-20
-10
0
10
20
Component 1

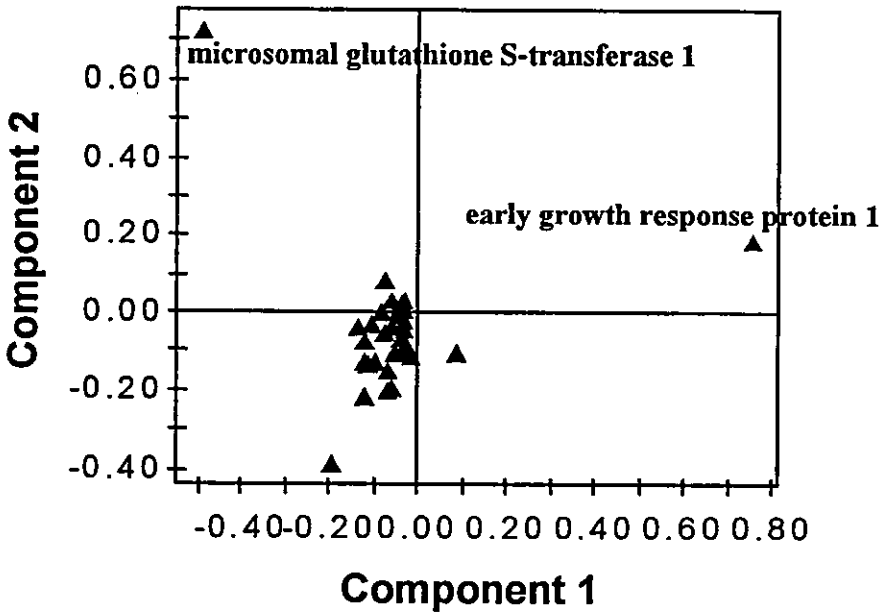
Component 2
0.60
0.40
0.20
0.00
-0.20
-0.40
microsomal glutathione S-transferase 1
early growth response protein 1
-0.40-0.200.00 0.20 0.40 0.60 0.80
Component 1

Fig 4

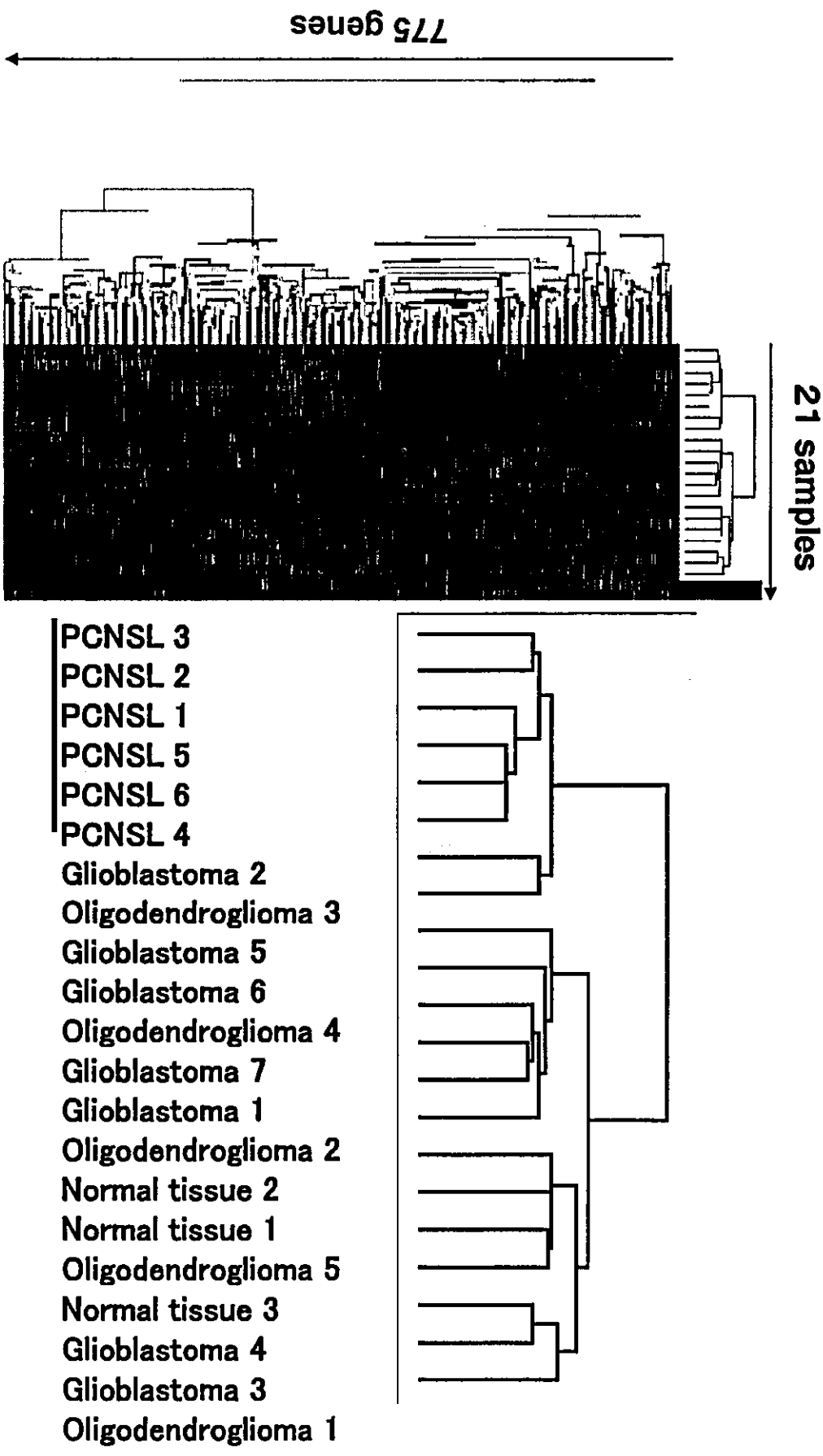
775 genes
21 samples
PCNSL 3
PCNSL 2
PCNSL 1
PCNSL 5
PCNSL 6
PCNSL 4
Glioblastoma 2
Oligodendroglioma 3
Glioblastoma 5
Glioblastoma 6
Oligodendroglioma 4
Glioblastoma 7
Glioblastoma 1
Oligodendroglioma 2
Normal tissue 2
Normal tissue 1
Oligodendroglioma 5
Normal tissue 3
Glioblastoma 4
Glioblastoma 3
Oligodendroglioma 1

Fig 5

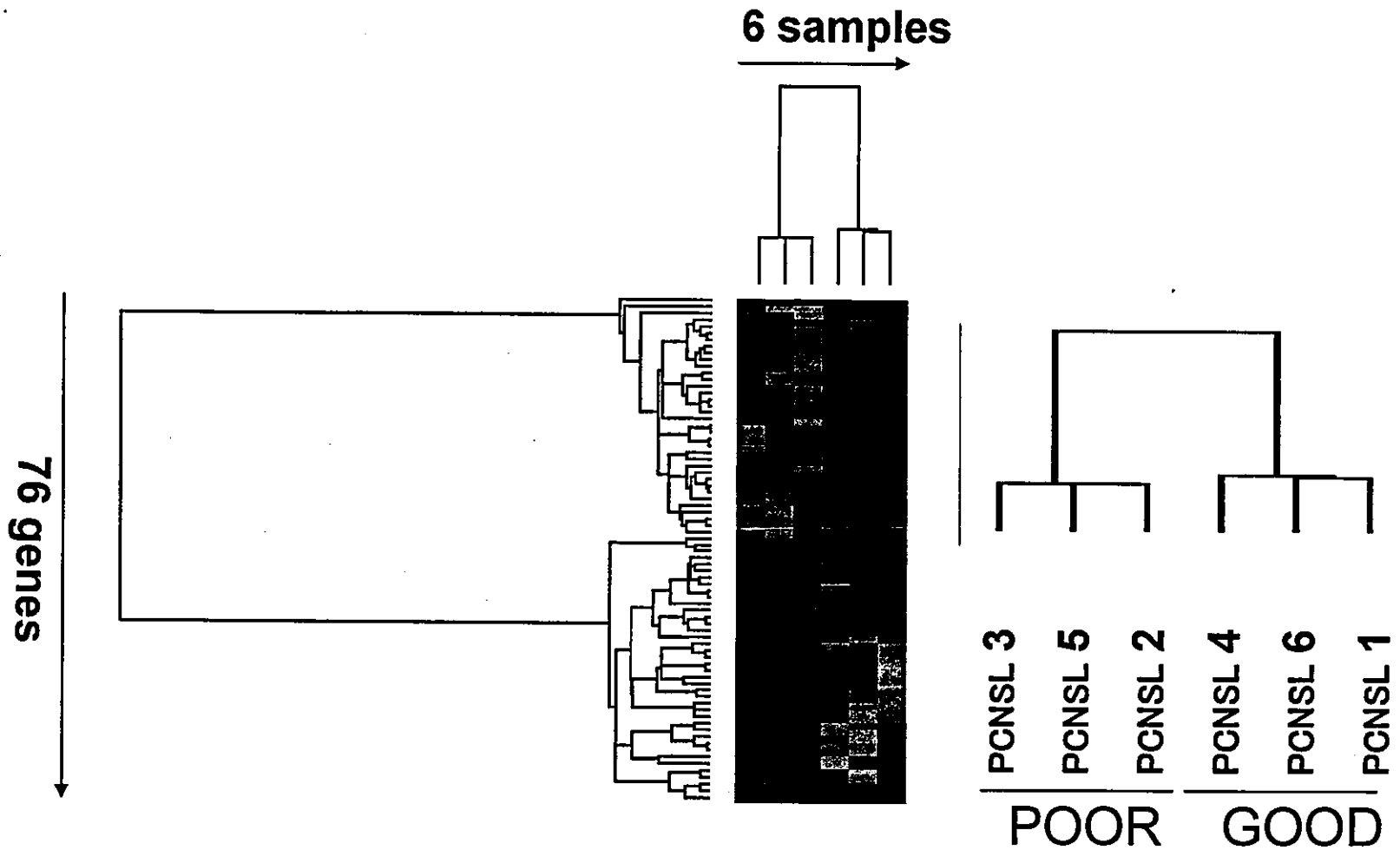
6 samples
76 genes
PCNSL 3
PCNSL 5
PCNSL 2
PCNSL 4
PCNSL 6
PCNSL 1
POOR
GOOD

Fig 6

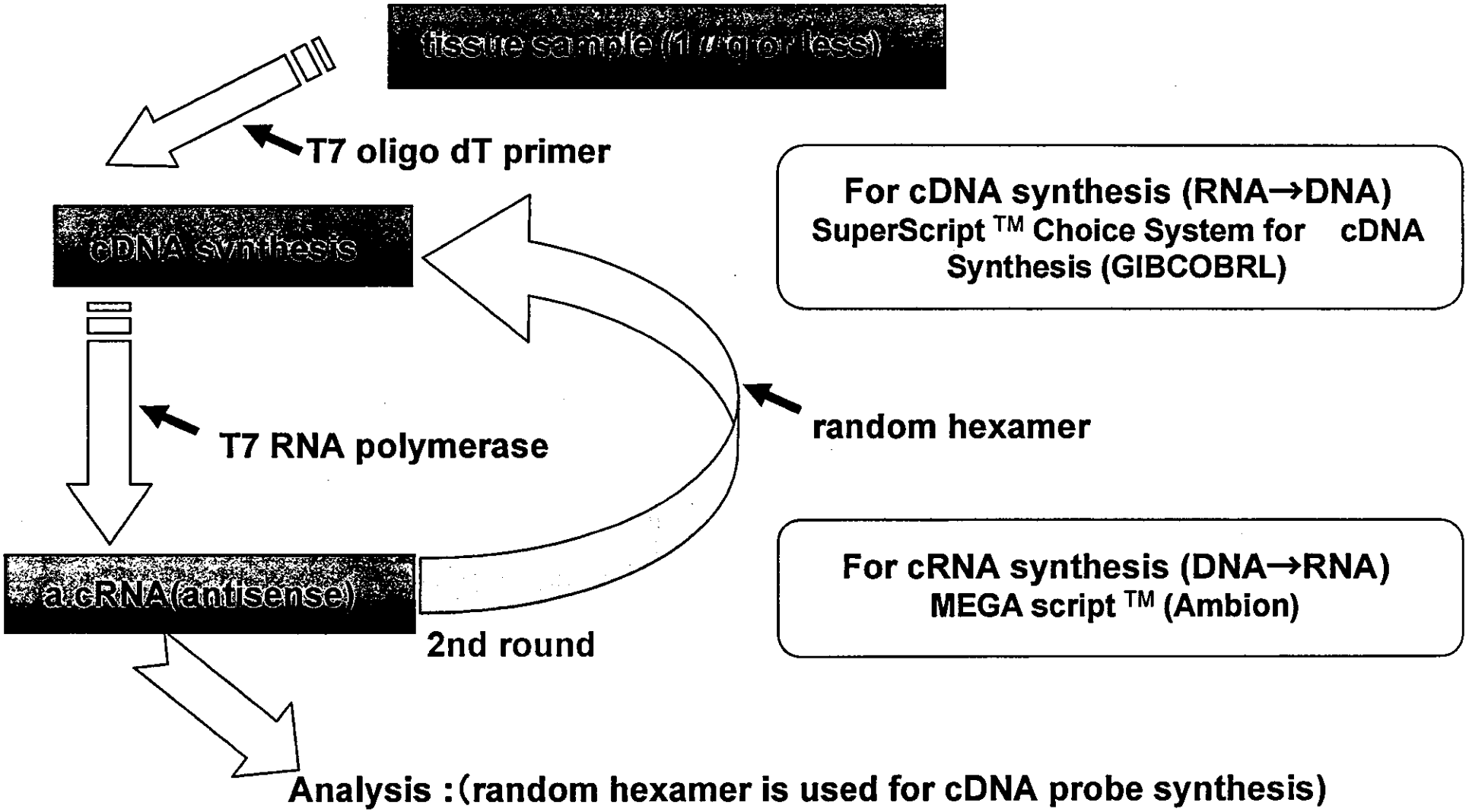
tissue sample (1 μg or less)
T7 oligo dT primer
cDNA synthesis
For cDNA synthesis (RNA→DNA)
SuperScript ™ Choice System for cDNA Synthesis (GIBCOBRL)
T7 RNA polymerase
random hexamer
a.cRNA(antisense)
2nd round
For cRNA synthesis (DNA→RNA)
MEGA script ™ (Ambion)
Analysis :(random hexamer is used for cDNA probe synthesis)

Fig 7

Is differential expression conserved even after amplification?

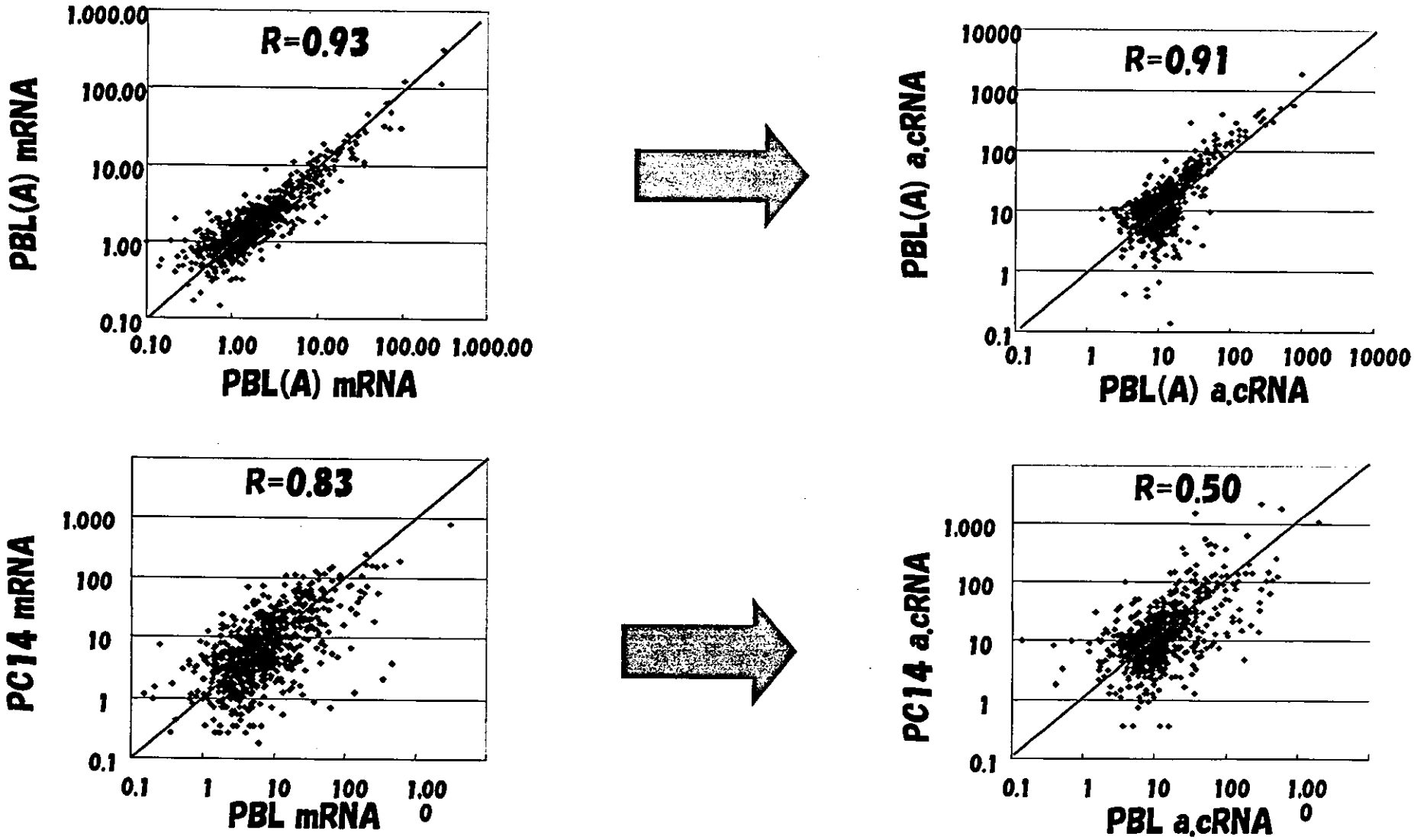

Fig 8

Experimental design and drawing PBL samples (tissue sample)

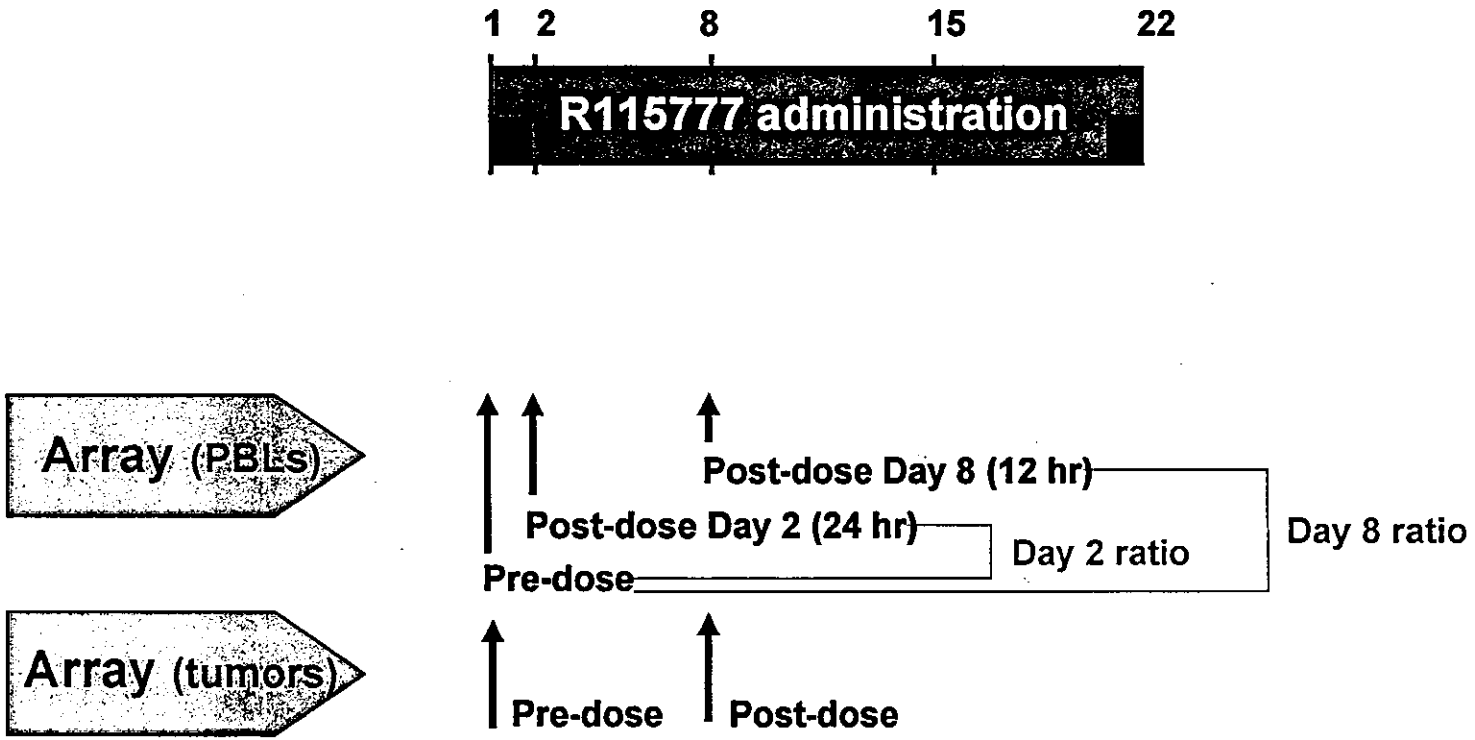

Fig.9 a

Custom Atlas™ Array (cDNA filter-array)

A set of 775 genes was chosen for predicting chemosensitivity analysis

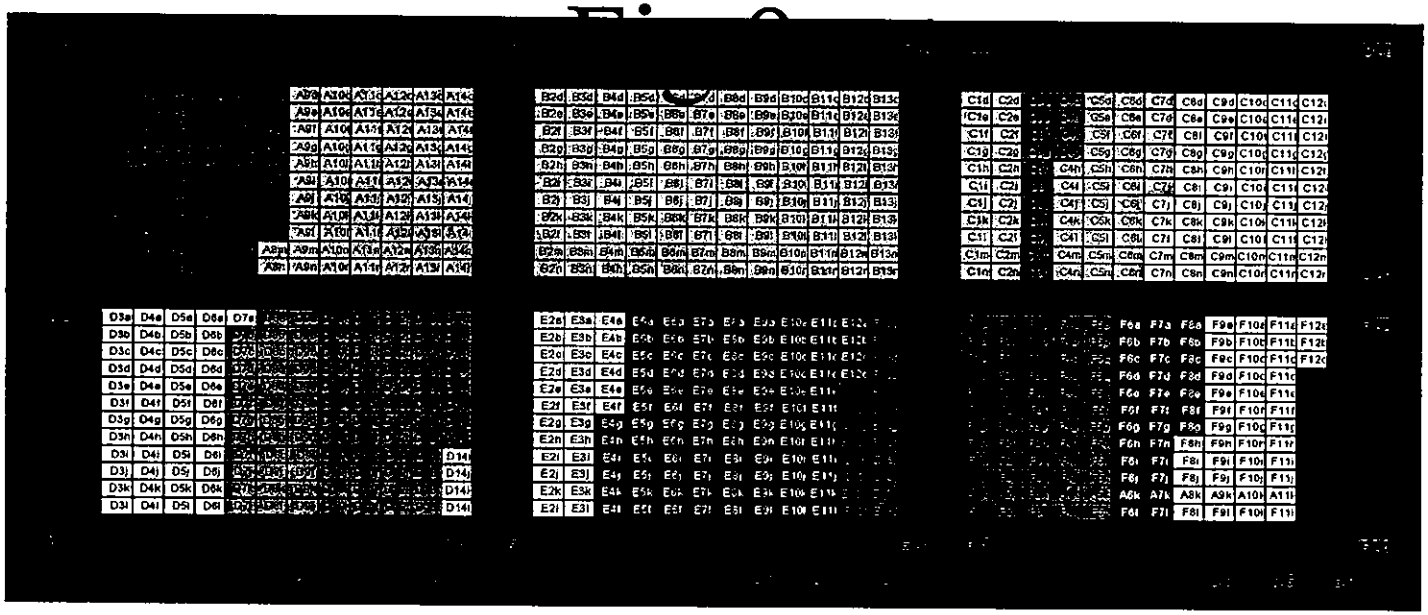

- 1: Cell Cycle Regulation
- 2: Signal / Oncogenes
- 3: Rho Family - Related Proteins
- 4: FTI - Related Proteins
- 5: Angiogenesis / Adhesion /Cell - Cell Interaction
- 6: Growth Factors
- 7: Cytokines
- 8: Apoptosis - Related Proteins
- 9: DNA Transcription Factors / Damage Response, Repair & Recombination
- 10: Metabolism
- 11: Translation / Protein Turnover / Detoxification Enzymes
- 12: Transporters / Nucleocytoplasmic Transporters / Symporters & Antiporters / Cytokeletal Proteins

Produced by Pharmacology Division, National Cancer Center Research Institute, Tokyo, Japan

Fig.9b

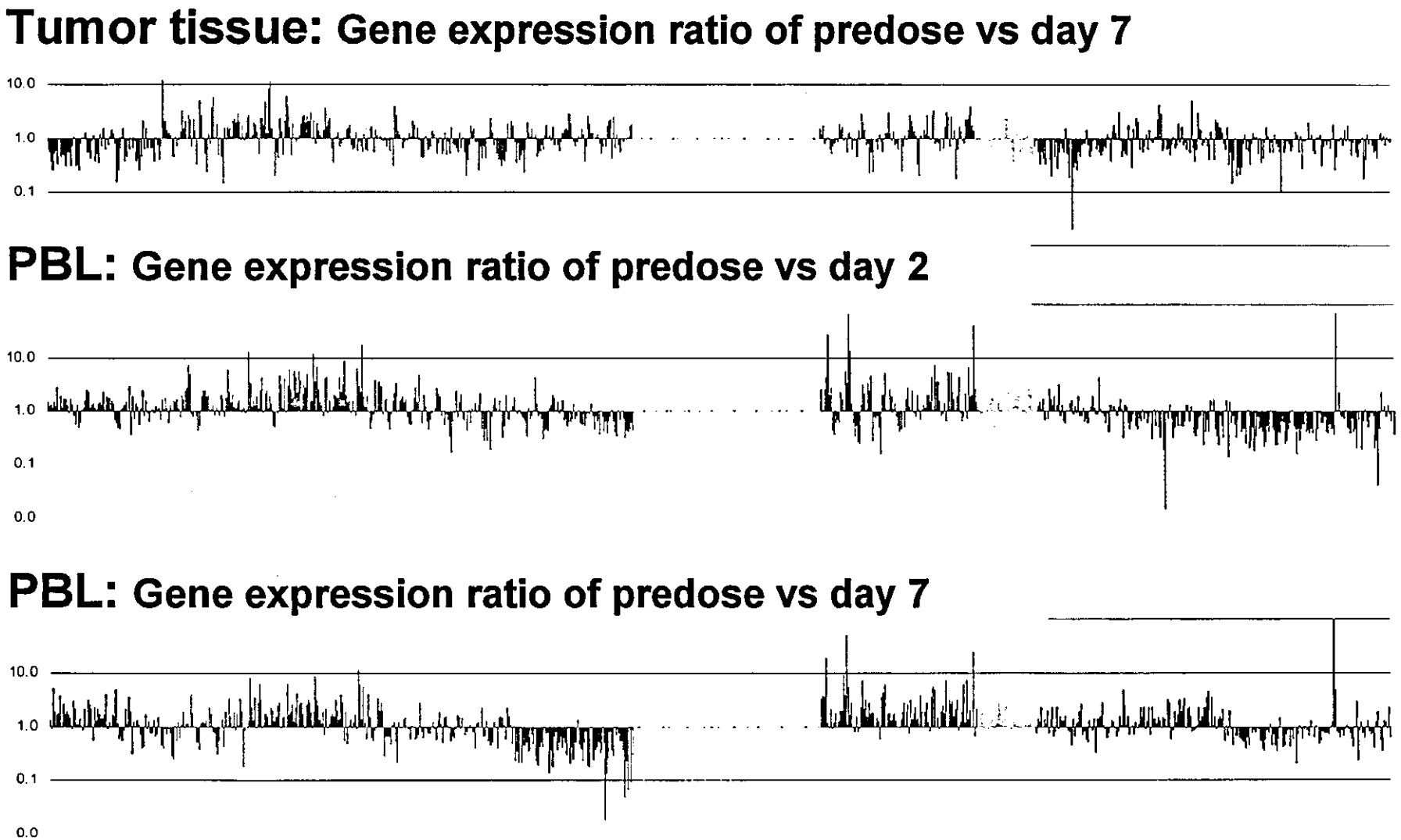
Tumor tissue: Gene expression ratio of predose vs day 7
10.0
1.0
0.1
PBL: Gene expression ratio of predose vs day 2
10.0
1.0
0.1
0.0
PBL: Gene expression ratio of predose vs day 7
10.0
1.0
0.1
0.0

Int. J. Cancer: **115**, 000–000 (2005)

Establishment of a human non-small cell lung cancer cell line resistant to gefitinib

Fumiaki Koizumi[1,3], Tatsu Shimoyama[1,4], Fumiko Taguchi[1,4], Nagahiro Saijo[2] and Kazuto Nishio[1,4]*
[1]*Shien-Lab, National Cancer Center Hospital, Tokyo, Japan*
[2]*Medical Oncology Department, National Cancer Center Hospital, Tokyo, Japan*
[3]*Investigative Treatment Division, National Cancer Center Institute EAST, Kashiwa, Japan*
[4]*Pharmacology Division, National Cancer Center Research Institute, Tokyo, Japan*

The epidermal growth factor receptor (EGFR) tyrosine-kinase inhibitor gefitinib (Iressa®, ZD1839) has shown promising activity preclinically and clinically. Because comparative investigations of drug-resistant sublines with their parental cells are useful approaches to identifying the mechanism of gefitinib resistance and select factors that determine sensitivity to gefitinib, we established a human non-small cell lung carcinoma subline (PC-9/ZD) that is resistant to gefitinib. PC-9/ZD cells are ~180-fold more resistant to gefitinib than their parental PC-9 cells and PC-9/ZD cells do not exhibit cross-resistance to conventional anticancer agents or other tyrosine kinase inhibitors, except AG-1478, a specific inhibitor of EGFR. PC-9/ZD cells also display significant resistance to gefitinib in a tumor-bearing animal model. To elucidate the mechanism of resistance, we characterized PC-9/ZD cells. The basal level of EGFR in PC-9 and PC-9/ZD cells was comparable. A deletion mutation was identified within the kinase domain of EGFR in both PC-9 and PC-9/ZD, but no difference in the sequence of EGFR cDNA was detected in either cell line. Increased EGFR/HER2 (and EGFR/HER3) heterodimer formations were demonstrated in PC-9/ZD cells by chemical cross-linking and immunoprecipitation analysis in cells unexposed to gefitinib. Exposure to gefitinib increased heterodimer formation in PC-9 cells, but not in PC-9/ZD cells. Gefitinib inhibits EGFR autophosphorylation in a dose-dependent manner in PC-9 cells but not in PC-9/ZD cells. A marked difference in inhibition of site-specific phosphorylation of EGFR was observed at Tyr1068 compared to other tyrosine residues (Tyr845, 992 and 1045). To elucidate the downstream signaling in the PC9/ZD cellular machinery, complex formation between EGFR and its adaptor proteins Grb2, SOS, and She was examined. A marked reduction in the Grb2-EGFR complex and absence of SOS-EGFR were observed in PC-9/ZD cells, even though the protein levels of Grb2 and SOS in PC-9 and PC-9/ZD cells were comparable. Expression of phosphorylated AKT was increased in PC-9 cells and inhibited by 0.02 μM gefitinib. But the inhibition was not significant in PC-9/ZD cells. These results suggest that alterations of adaptor-protein-mediated signal transduction from EGFR to AKT is a possible mechanism of the resistance to gefitinib in PC-9/ZD cells. These phenotypes including EGFR–SOS complex and heterodimer formation of HER family members are potential biomarkers for predicting resistance to gefitinib.
© *2005 Wiley-Liss, Inc.*

Key words: resistance; gefitinib; EGFR; Grb2; SOS; non-small cell lung cancer

Chemotherapy has played a central role in the treatment of patients with inoperable NSCLC for over 30 years, although its efficacy seems to be of very limited value.[1,2] Human solid tumors, including lung cancer, glioblastoma, breast cancer, prostate cancer, gastric cancer, ovarian cancer, cervical cancer and head and neck cancer, express epidermal growth factor receptor (EGFR) frequently, and elevated EGFR levels are related to disease progression, survival, stage and response to therapy.[2–10] The therapies directed at blocking EGFR function are attractive.

Interest in target-based therapy has been growing ever since the clinical efficacy of STI-571 was first demonstrated,[11–13] and small molecules and monoclonal antibodies that block activation of the EGFR and ErbB2 have been developed over the past few decades. The leading small-molecule EGFR tyrosine-kinase inhibitor, gefitinib (Iressa®, ZD1839), has shown excellent antitumor activity in a series of Phase I and II studies,[14,15] and Phase II international multicenter trials (IDEAL1 and 2) yield an overall RR of 11.8–18.4% and overall disease control rate of 42.2–54.4% (gefitinib 250 mg/day) in patients with advanced non-small cell lung cancer (NSCLC) who had undergo at least 2 previous treatments with chemotherapy. INTACT 1 and 2 ('Iressa' NSCLC Trials Assessing Combination Therapy) have demonstrated that gefitinib does not provide improvement in survival when added to standard first line platinum-based chemotherapy *vs.* chemotherapy alone in advanced NSCLC.[16,17] Two small retrospective studies reported recently that activating mutation of EGFR correlate with sensitivity and clinical response to gefitinib and erlotinib.[18–20] Although information of EGFR mutation may enable to identify the subgroup of patients with NSCLC who will respond to gefitinib and erlotinib, it would be expected that acquired resistance would develop in such patients after treatment. The problem of acquired resistance to gefitinib might be growing, but there has been no preclinical research about the mechanism of developing resistance to gefitinib. We established resistant subline using PC-9 that is highly sensitive to gefitinib.

Establishment of drug-resistant sublines and comparative investigations with their parental cells to identify their molecular, biological and biochemical properties are useful approaches to elucidating the mechanism of the drug's action. Our study describes the establishment of a gefitinib-resistant cell line and its characterization at the cellular and subcellular levels. The PC-9/ZD cell line is the first human NSCLC cell line resistant to gefitinib ever reported. PC-9 is a lung adenocarcinoma cell line that is highly sensitive to gefitinib at its IC_{50}-value of 0.039 μM, but the PC-9/ZD subline, which has a level of EGFR expression comparable to that of PC-9 cells, is specifically resistant to gefitinib. Thus, PC-9 and PC-9/ZD cells will provide useful information about the mechanism of developing resistance to gefitinib and molecules as surrogate markers for predicting chemosensitivity to gefitinib.

Material and methods

Drugs and cells

Gefitinib(*N*-(3-chloro-4-fluorophenyl)-7-methoxy-6-[3-(morpholin-4-yl)propoxy] quinazolin-4-amine) was supplied by AstraZeneca Pharmaceuticals (Cheshire, UK). AG-1478, AG-825, K252a, staurosporin, genistein, RG-14620 and Lavendustin A were purchased from Funakoshi Co. Ltd (Tokyo, Japan).

NSCLC cell line PC-9 (derived from a patient with adenocarcinoma untreated previously) was provided by Prof. Hayata of Tokyo Medical University (Tokyo, Japan).[21] PC-9 and PC-9/ZD cells were cultured in RPMI-1640 medium (Sigma, St. Louis, MO) supplemented with 10% FBS (GIBCO-BRL, Grand Island, NY), penicillin and streptomycin (100 U/ml and 100 μg/ml, respectively; GIBCO-BRL) in a humidified atmosphere of 5% CO_2 at 37°C. Gefitinib-resistant PC-9/ZD cells were selected from

*Correspondence to: Shien-Lab, Medical Oncology Department, National Cancer Center Hospital, 5-1-1 Tsukiji, Chuo-ku, Tokyo, 104-0045, Japan. Fax: 181-3-3547-5185. E-mail: knishio@gan2.res.ncc.go.jp
Received 1 July 2004; Accepted after revision 21 December 2004
DOI 10.1002/ijc.20985
Published online 00 Month 2005 in Wiley InterScience (www.interscience.wiley.com).

J_ID: Z3Q Customer A_ID: 04-1248 Cadmus Art: IJC5519 Date: 22-FEBRUARY-05 Stage: I

a subculture that had acquired resistance to gefitinib using the following procedure. Cultured PC-9 cells were exposed to 2.5 μg/ml *N*-methyl-*N'*-nitro-*N*-nitrosoguanidine (MNNG) for 24 hr and then washed and cultured in medium containing 0.2 μM gefitinib for 7 days. After exposure to gefitinib, they were washed and cultured in drug-free medium for 14 days. When variable cells had increased, they were seeded in medium containing 0.3–0.5 μM of gefitinib on 96-well cultured plates for subcloning. After 21–28 days, the colonies were harvested and a single clone was obtained. The subcloned cells exhibited an 182-fold increase in resistance to the growth-inhibitory effect of gefitinib as determined by MTT assay, and the resistant phenotype has been stable for at least 6 months under drug-free conditions.

In vitro *growth-inhibition assay*

The growth-inhibitory effects of cisplatin, carboplatin, adriamycin, irinotecan, gemcitabine, vindesine, paclitaxel, genistein, K252a, staurosporin, AG-825, AG-1478, Tyrophostin 51, RG-14620, Lavendustin A and gefitinib in PC-9 and PC-9/ZD cells were examined by using a 3-(4,5-dimethylthiazol-2-yl)- 2,5-diphenyltetrazolium bromide (MTT) assay.[22] A 180 μl volume of an exponentially growing cell suspension (6×10^3 cells/ml) was seeded into a 96-well microtiter plate, and 20 μl of various concentrations of each drug was added. After incubation for 72 hr at 37°C, 20 μl of MTT solution (5 mg/ml in PBS) was added to each well, and the plates were incubated for an additional 4 hr at 37°C. After centrifuging the plates at 200*g* for 5 min, the medium was aspirated from each well and 180 μl of DMSO was added to each well to dissolve the formazan. Optical density was measured at 562 and 630 nm with a Delta Soft ELISA analysis program interfaced with a Bio-Tek Microplate Reader (EL-340, Bio-Metallics, Princeton, NJ). Each experiment was carried out in 6 replicate wells for each drug concentration and carried out independently 3 or 4 times. The IC_{50} value was defined as the concentration needed for a 50% reduction in the absorbance calculated based on the survival curves. Percent survival was calculated as: (mean absorbance of 6 replicate wells containing drugs − mean absorbance of six replicate background wells)/(mean absorbance of 6 replicate drug-free wells − mean absorbance of 6 replicate background wells) × 100.

In vivo *growth-inhibition assays*

Experiments were carried out in accordance with the United Kingdom Coordinating Committee on Cancer Research Guidelines for the welfare of animals in experimental neoplasia (2nd ed.). Female BALB/c nude mice, 6-weeks-old, were purchased from Japan Charles River Co. Ltd (Atsugi, Japan). All mice were maintained in our laboratory under specific-pathogen-free conditions. *In vivo* experiments were scheduled to evaluate the effect of oral administration of gefitinib on pre-existing tumors. Ten days before administration, 5×10^6 PC-9 or PC-9/ZD cells were injected subcutaneously (s.c.) into the back of the mice, and gefitinib (12.5, 25 or 50 mg/kg, p.o.) was administered to the mice on Days 1–21. Tumor diameter was measured with calipers on Days 1, 4, 8, 11, 14, 19 and 22 to evaluate the effect of treatment, and tumor volume was determined by using the following equation: tumor volume = $ab^2/2$ (mm^3) (where *a* is the longest diameter of the tumor and *b* is the shortest diameter). Day "x" denotes the day on which the effect of the drugs was estimated, and Day "1" denotes the first day of treatment. All mice were sacrificed on Day 22, after measuring their tumors. We considered absence of a tumor mass on Day 22 to indicate a cure. Differences in tumor sizes between the treatment groups and control group at Day 22 were analyzed by the unpaired *t*-test. A *p*-value of <0.05 was considered statistically significant.

cDNA expression array

The gene expression profile of PC-9/ZD was assessed with an Atlas Nylon cDNA Expression Array (BD Bioscience Clontech, Palo Alto, CA). Total RNA was extracted by a single-step guanidinium thiocyanate procedure (ISOGEN, Nippon Gene, Tokyo, Japan). An Atlas Pure Total RNA Labeling System was used to isolate RNA and label probes. The materials provided with the kit were used, and the manufacturer's instructions were followed for all steps. Briefly, streptavidin-coated magnetic beads and biotinylated oligo(dT) were used to isolate poly A RNA from 50 μg of total RNA and the RNA obtained was converted into ^{32}P-labeled first-strand cDNA with MMLV reverse transcriptase. The ^{32}P-labeled cDNA fraction was purified on NucleoSpin columns and was added to the membrane on which fragments of 777 genes were spotted. Hybridization was allowed to proceed overnight at 68°C. After washing, the radiolabeled spots were visualized and quantified by BAS-2000II and Array Gauge 1.1 (Fuji Film Co., Ltd., Tokyo, Japan). The data were adjusted for the total density level of each membrane.

Quantitative Real-Time RT-PCR Analysis

Total RNAs extracted from PC-9 cells and PC-9/ZD cells (1×10^6 cells each) were incubated with DNase I (Invitrogen) for 30 min. First-strand cDNA synthesis was carried out on 1 μg of RNA in 10 μl of a reaction mixture with 50 pmol of Random hexamers and 50 U of M-MLV RTase. Oligonucleotide primers for human EGFR were obtained from Takara (HA003051, Takara Bio Co., Tokyo, Japan). For PCR calibration, we generated a calibrator dilution series for EGFR cDNA in pUSEamp vector (Upstate, Charlottesville, VA) ranging from 10^8–10^2 copies/1 μl. A total of 2 μl of reverse transcriptase products was used for PCR amplification using Smart Cycler system (Takara) according to manufacturer's instructions. Absolute copy numbers were calculated back to the initial cell numbers, which were set into the RNA extraction. As a result we obtained copies/cell:ratio representing the average EGFR RNA amount per cell.

Immunoprecipitation and immunoblotting

The cultured cells were washed twice with ice-cold PBS, and lysed in EBC buffer (50 mM Tris-HCl, pH 8.0, 120 mM NaCl, 0.5% Nonidet P-40, 100 mM NaF, 200 mM Na orthovanadate, and 10 mg/ml each of leupeptin, aprotinin, pepstatin A and phenylmethylsulphonyl fluoride). The lysate was cleared by centrifugation at 15,000 r.p.m. for 10 min, and the protein concentration of the supernatant was measured by BCA protein assay (Pierce, Rockford, IL). The membrane was probed with antibody against EGFR (1005; Santa Cruz, Santa Cruz, CA), HER2/neu (c-18; Santa Cruz), HER3 (c-17; Santa Cruz), HER4 (c-18; Santa Cruz), PI3K (4; BD), Grb2 (81; BD), SOS1/2 (D-21; Santa Cruz), Shc (30; BD, San Jose, CA), PTEN (9552; Cell Signaling, Beverly, MA), AKT (9272; Cell Signaling), phospho-EGFR specific for Tyr 845, Tyr 992, Tyr 1045, and Tyr 1068 (2231, 2235, 2237, 2234; Cell Signaling), phospho-AKT (Ser473) (9271; Cell Signaling), phospho-Erk (9106; Cell Signaling), and phospho-Tyr (PY-20; BD) as the first antibody, and then with by horseradish-peroxidase-conjugated secondary antibody. The bands were visualized by enhanced chemiluminescence (ECL Western Blotting Detection Kit, Amersham, Piscataway, NJ). For Immunoprecipitation, 5×10^6 cells were washed, lysed in EBC buffer, and centrifuged, and the supernatants obtained (1,500 μg) were incubated at 4°C with the anti-EGFR (1005), -HER2 (c-18), and -HER3 (c-17) Ab overnight. The immunocomplexes were absorbed onto protein A/G-Sepharose beads, washed 5 times with lysate buffer, denatured, and subjected to electrophoresis on a 7.5% polyacrylamide gel.

Analysis of the genes of the HER families by direct sequencing

Total RNAs were extracted from PC-9 and PC-9/ZD cells with ISOGEN (Nippon Gene) according to manufacturer's instructions. First-strand cDNA was synthesized from 2 μg of total RNA by using 400 U of SuperScript II (Invitrogen, Carlsbad, CA). After reverse transcription with oligo (dT) primer (Invitrogen) or random primer (Invitrogen), the first-strand cDNA was amplified by PCR by using specific primers for EGFR, HER2 and HER3. The

J_ID: Z3Q Customer A_ID: 04-1248 Cadmus Art: IJC5519 Date: 22-FEBRUARY-05 Stage: I

reaction mixture (50 µl) contained 1.25 U AmpliTaq DNA polymerase (Applied Biosystem, Foster City, CA), and amplification was carried out by 30 cycles of denaturation (95°C, 30 sec), annealing (55–59°C, 30 sec), and extension (72°C, 30 sec) with a GeneAmp PCR System 9600 (Applied Biosystem). After amplification, 5 µl of the RT-PCR products was subjected to electrophoretic analysis on a 2% agarose gel with ethidium bromide. DNA sequencing of the PCR products was carried out by the dideoxy chain termination method using the ABI PRISM 310 Genetic Analyzer (Applied Biosystem).

Chemical cross-linking

Chemical cross-linking in intact cells was carried out as described previously.[23] In brief, after 6 hr exposure to 0.2 µM gefitinib, cells were washed with PBS and incubated for 25 min at 4°C in PBS containing 1.5 mM of the nonpermeable cross-linker bis (sulfosuccinimidyl) substrate (Pierce, Rockford, IL). The reaction was terminated by adding 250 mM glycine for 5 min while rocking. Cells were washed in EBC buffer and 20 µg of protein was resolved by 5–10% gradient SDS-PAGE, and then immunoblot analyzed for EGFR, HER2, HER3 and P-Tyr.

Results

Sensitivity of PC-9/ZD cells to cytotoxic agents and tyrosine kinase inhibitors

No significant difference between PC-9 and PC-9/ZD cells was observed in *in vitro* cell growth (doubling time of 20.3 hr and 21.4 hr, respectively) and microscopic morphology. Figure 1 shows the growth-inhibitory effect of gefitinib on the parent PC-9 cell line and its resistant subline, PC-9/ZD. The IC_{50}-value of gefitinib in PC-9 cells was 0.039 µM, as compared to 7.1 µM in PC-9/ZD cells (182-fold resistance). PC-9/ZD cells exhibited no cross-resistance to other conventional anticancer agents, including cisplatin, carboplatin, adriamycin, vindesine, paclitaxel and irinotecan. We also examined the growth-inhibitory effect of the EGFR tyrosine kinase inhibitors AG-1478, RG-14620 and Lavendustin A and other tyrosine kinase inhibitors in PC-9 and PC-9/ZD cells. PC-9/ZD cells show cross-resistance to AG1478, but not to all of the tyrosine kinase inhibitors (Tables I, II). It is likely that PC-9/ZD would also be resistant to EGFR-targeted quinazoline derivatives including gefitinib and erlotinib.[20]

PC-9/ZD cells show significant resistance to gefitinib in an in vivo model

To ascertain whether the resistance of PC-9/ZD occurs *in vivo*, we investigated the growth-inhibitory effect of gefitinib on PC-9 cells and PC-9/ZD cells in a xenotransplanted model. There was no significant difference in the size of the of PC-9 and PC-9/ZD cell tumor masses in nude mice before the start of gefitinib injection. Figure 2 shows the growth-inhibition curve of PC-9 (Fig. 2*a*) and PC-9/ZD (Fig. 2*b*) cells *in vivo* during the observation period. The PC-9 tumor masses decreased markedly in volume at all doses of gefitinib. In the 50 mg/kg/day p.o. group, the PC-9 masses were eradicated in all mice and did not regrow within the observation period. Growth of the PC-9/ZD masses, on the other hand, was inhibited by gefitinib administration in a dose-dependent manner, but significant tumor reduction was observed only in the 25 and 50 mg/kg/day groups, and the PC-9/ZD masses were not eradicated even in 50 mg/kg/day group. These results clearly demonstrate the significant *in vivo* resistance of PC-9/ZD cells to gefitinib.

Expression of HER family members and related molecules in PC-9 and PC-9/ZD cells

We examined the gene expression and protein levels of HER family members and related molecules by cDNA expression array (followed by confirmation using RT-PCR, data not shown) and immunoblotting. The ratios of the protein expression levels of PC-9 cells to PC-9/ZD cells almost paralleled the expression levels of their genes (Fig. 3*a*). The basal level of EGFR was comparable or slightly higher in PC-9/ZD cells (Fig. 3*a,b*), whereas the HER3 and AKT levels were lower in resistant cells.

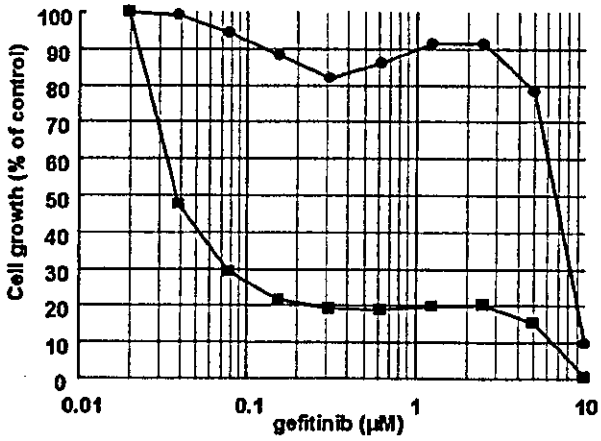

	PC-9	PC-9/ZD
IC_{50} value (µM)	0.039 ± 0.002	7.1 ± 0.06
Doubling time (hr)	20.3	21.0

FIGURE 1 – Growth-inhibitory effect of gefitinib on PC-9 and PC-9/ZD cells determined by MTT assay. The cells were exposed to the concentrations of gefitinib indicated for 72 hr. The growth–inhibition curves of PC-9 (■) and PC-9/ZD (●) are shown. Doubling time was determined by MTT assay.

TABLE I – CHEMOSENSITIVITY TO OTHER ANTICANCER DRUGS

Drug	IC_{50} values (µM)[1]		RR[2] 1 6
	PC-9	PC-9/ZD	
Cisplatin	1.9 ± 0.7	3.1 ± 1.5	2.0
Carboplatin	25 ± 21	49 ± 23	1.3
Adriamycin	0.16 ± 0.13	0.20 ± 0.15	2.2
Irinotecan	15 ± 10	32 ± 11	1.5
Etoposide	4.5 ± 1.5	6.6 ± 1.3	1.5
Gemcitabine	18 ± 1.5	27 ± 1.5	0.7
Vindesine	0.0046 ± 0.0004	0.0032 ± 0.0009	1 2
Paclitaxel	0.0041 ± 0.0011	0.0048 ± 0.0004	1.6

[1]As assessed by MTT assay in PC-9 and PC-9/ZD cells. Values are the mean ± SD of >3 independent experiments.–[2]Relative resistance value (IC_{50} of resistant cells/IC_{50} of parental cells).

We carried out quantitative RT-PCR to measure the copy numbers of EGFR. Estimated transcript levels of EGFR were 786.3 and 712.1 copies/cell for PC-9 cells and PC-9/ZD cells, respectively (Fig. 3*d*). Relative ratio of EGFR expression levels in PC-9 cells and PC-9/ZD cells is 1.104. Microarray analysis using CodeLink Bioarray (Amersham Bio, Piscataway, NJ) confirmed equivalent gene expression of EGFR with ratio of 1.002 between PC-9 and PC-9/ZD cells (data not shown).

Expression of PI3K, Grb2, SOS, and Shc, the adaptor proteins of EGFR, and PTEN was almost the same in PC-9 and PC-9/ZD cells, and no change in the protein levels was observed after exposure to gefitinib (data not shown). The relative densitometric units of each protein are shown in Figure 3*c*. These results suggest that the difference in protein levels of EGFR, HER2, and related proteins can not explain the high resistance of PC-9/ZD cells to gefitinib.

Sequence of HER family member in PC-9/ZD cells

Several reports suggest that the resistance to receptor tyrosine kinase inhibitor STI-571 is partially due to mutations in the